Medium Range Ordering realized in $Zr_{80}Pt_{20}$Amorphous Alloy

K Sugiyama, T Kawamata and T Muto

Institute for Materials Research (IMR), Tohoku University, Sendai 980-8577, Japan

The corresponding author's e-mail address: kazumasa@imr.tohoku.ac.jp

Abstract. The short- and medium-range ordering structure in $Zr_{80}Pt_{20}$ amorphous alloy has been investigated by anomalous X-ray scattering coupled with reverse Monte-Carlo simulation. Pt prefers to construct a Zr-rich icosahedral complex with unique chemical and topological short-range ordering. The present analysis also revealed the medium-range ordering of Pt-Pt pairs corresponding to the pre-peak signal at 17 nm^{-1} in the diffraction profile. The chemical and topological features around Pt and bonding structure correspond well with those of Mn in the approximant phase of α-AlMnSi.

1. Introduction

The short- to medium-range atomic ordering in amorphous alloys has attracted considerable attention because the interesting properties of amorphous alloys are closely associated with their atomic arrangement. Previous structural reports of Zr-based amorphous alloys have introduced an icosahedral-like atomic arrangement. It has been recognized that this structural feature improves the stability of the super-cooled liquid state and also promotes the formation of nano-sized quasicrystals [1]. The study of Zr-Pt and Zr-Pd amorphous alloys suggested that the formation of the icosahedral phase was attributed to possible icosahedral medium-range ordering (MRO) [2]. In particular, further X-ray absorption fine structure (XAFS) analysis of $Zr_{80}Pt_{20}$ amorphous alloys led to an interesting suggestion that the unique local structure around Pt is a key to elucidating the properties of the $Zr_{80}Pt_{20}$ amorphous alloy [3]. Simultaneously, the Pt-rich Zr-Pt amorphous alloy exhibited a pre-peak signal at about Q = ~17 nm^{-1}, and the pre-peak was suggested to be related to the medium-range order comprised by Pt-centered clusters [4, 5]. In these contexts, it was concluded that the $Zr_{80}Pt_{20}$ amorphous structure comprises icosahedral MRO related to the Pt-centered cluster. This prompts us to apply the state of the art anomalous X-ray scattering (AXS) technique coupled with reverse Monte Carlo (RMC) simulation [6] for the analysis of the $Zr_{80}Pt_{20}$ amorphous alloy. AXS analysis utilizing the anomalous dispersion effect near the absorption edge provides environmental structural information about Zr and Pt. That analysis, combined with RMC simulation, allows us to discuss the three-dimensional (3D) atomic configuration of the amorphous structure.

2. Experimentals

$Zr_{80}Pt_{20}$ amorphous ribbons of approximately 20 μm thickness and 2 mm width were produced by the single roller melt-spinning technique in an Ar atmosphere. The density of the amorphous ribbon sample, measured by Archimedes' method, was 8.74 Mg/m^3. AXS measurements at the Pt L_3 absorption edge were carried out at the beam line station 7C, Institute of Materials Structure Science, High Energy Accelerator Research Organization, Tsukuba, Japan. AXS measurements at the Zr K absorption edge were carried out at the beam line station NW10A. Each pair of incident energies, corresponding to 25 eV and 300 eV below the absorption edge, was used in the present AXS measurements, and the anomalous dispersion terms for Pt and Zr were calculated using the relativistic Cromer and Liberman method [7]. After correcting for absorption and fluorescent radiation, the observed intensity was subsequently converted to electron units per atom using the generalized Krogh–Moe–Norman method. The Compton scattering effect was considered by using the theoretical values for a free atom with the so-called Breit–Dirac recoil factor. For the RMC simulation, we started

with an initial model of 20,000 atoms (Zr: 16000 and Pt: 4000) with a dense random packing (DRP) structure in a cubic hyper-cell with a unit size of L = 8.102 nm.

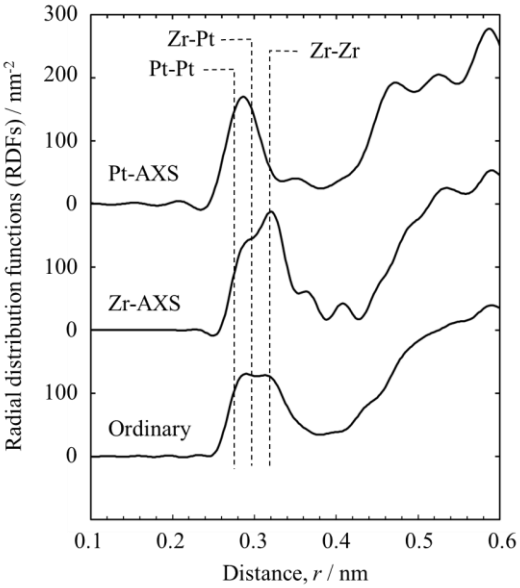

Figure 1. Ordinary- and environmental- RDFs around Pt and Zr of $Zr_{80}Pt_{20}$. Ordinary RDF was obtained from the intensity profile measured at 17.699 keV.

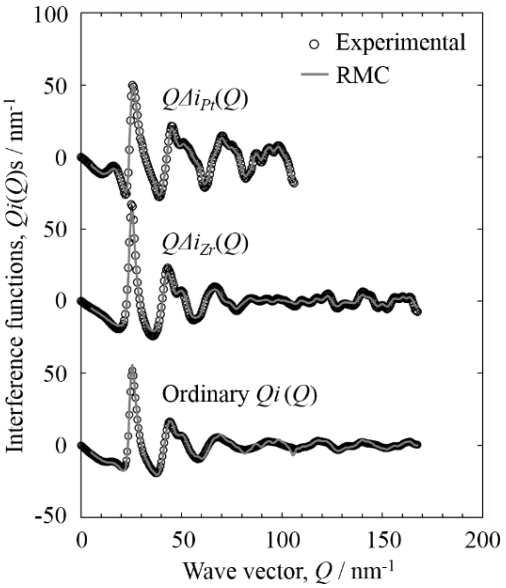

Figure 2. Ordinary- and environmental-interference functions. The solid line and dots correspond to the experimental and AXS-RMC simulation, respectively.

3. Results and Discussion

Figure 1 shows the ordinary RDF and environmental RDFs around Zr and Pt obtained by AXS measurements. The vertical dashed lines indicate the nearest neighbor atomic distances for Pt-Pt, Zr-Pt, and Zr-Zr pairs (Pt-Pt: 0.276 nm, Zr-Pt: 0.298 nm, Zr-Zr: 0.320 nm) estimated from the Goldschmidt radii. The pair correlation corresponding to the nearest Zr-Zr pair around 0.320 nm disappears in the environmental RDF around Pt. The environmental RDF around Zr indicates two types of pair correlations of Zr-Pt and Zr-Zr pairs. The observed first-nearest Zr-Pt distance is in the intermediate region between the distances for Pt-Pt and Zr-Pt pairs estimated from the Goldschmidt radii. This short Zr-Pt inter-atomic distance corresponds well with the small mixing enthalpy between Zr and Pt (−100 kJ/mol) [8]. It is interesting to note some features found in the experimental interference functions in Figure 2. A pre-peak signal is observed at approximately Q = 17 nm^{-1} in the functions of $Qi(Q)$ and $Q\Delta i_{Pt}(Q)$, but not in the function of $Q\Delta i_{Zr}(Q)$. This result also suggests that the pre-peak originates from the Pt-Pt interaction in the medium-range correlation. The excellent agreement between the experimentally obtained $Q\Delta i_{Pt}(Q)$, $Q\Delta i_{Zr}(Q)$, and $Qi(Q)$ and that of the RMC structural model, including the pre-peak signal, indicates that the structural model is extremely useful for the discussion of elemental selectivity and MRO. The structural parameters of averaged atomic distance and coordination number as well as other key parameters in the nearest neighbor region are summarized in Table 1. The structural information for the Zr-Pt pair suggests that there is high chemical affinity between Pt and Zr in the first-nearest Pt-Zr pair. As an example, the short distance of p_{PtZr} in comparison with that estimated from the Goldschmidt radii, clearly suggest the chemically strong bond associated with the small mixing enthalpy between Zr and Pt. In order to evaluate the topological features in the first-neighbor region, Voronoi polyhedral analysis was carried out.

Table 1 The short range ordering found in amorphous $Zr_{80}Pt_{20}$ alloy. (The averaged atomic distance, r_{ij}, the first peak top position p_{ij} , the averaged coordination number Z_{ij}, and chemical occupancy in the nearest neighbor region.)

i	*j*	r_{ij} [nm]	p_{ij} [nm]	Z_{ij}	Occup.(%)
Zr	Zr	0.327	0.319	11.3	82.5
	Pt	0.311	0.282	2.4	17.5
				13.7	
Pt	Zr	0.311	0.282	9.5	86.4
	Pt	0.284	0.270	1.5	13.6
				11.0	

Figure 3 shows the frequency distribution of typical Voronoi indices of Pt observed in the $Zr_{80}Pt_{20}$ amorphous alloy. The topological features around Zr are rather featureless and reproduced well by the DRP model. On the other hand, Pt has a strong preference for short-range ordering (SRO) in an icosahedron-like fashion, (0 2 8 2 0) and (0 2 8 1 0). This result allows us to consider the present Pt-centered icosahedral SRO as one of the most important structural units driven by the strong chemical affinity of the Pt-Zr pairs. The present structural analysis of the SRO in the first-nearest-neighbor region is useful for understanding the fundamental structural features in amorphous alloys; however, it is sometimes necessary to extend the model to the second-nearest-neighbor region. The present case of the $Zr_{80}Pt_{20}$ amorphous alloy could be included in this category because the pre-peak signal associated with the enhanced correlation at approximately 0.45 nm is due to the Pt-Pt correlation. The common-neighbor analysis (CNA) [9] is useful for this purpose, and the present paper demonstrates the results of the CNA for the MRO of such a Pt-Pt correlation. Figure 4 shows the results of CNA for the Pt-Pt root pairs in the second peak of the partial $g_{PtPt}(r)$. The root-pairs in this region were ranked mainly into three CNA indices of $[333]_{CN}$, $[322]_{CN}$, and $[211]_{CN}$ and the three connections indicate the remarkably higher Zr population in the common neighbors. This result readily suggests that the second-nearest Pt-Pt pairs closely associated with the pre-peak signal accommodate common neighbors of Zr rather than Pt so as to produce Zr-rich chemical short-range ordering around Pt. It may be interesting to compare the structural features of $Zr_{80}Pt_{20}$ with those of the α-AlMnSi approximant with a typical Mackay cluster [10]. Voronoi polydehdral analysis around Mn in α-AlMnSi indicates the preference for the icosahedral-like arrangement of Al with Voronoi indices of (0 0 12 0 0) and (0 2 8 2 0). At the same time, connections with the indices $[333]_{CN}$ is also common for MRO for the Mn-Mn root pairs. The similarity between the structure around Pt in $Zr_{80}Pt_{20}$ amorphous alloy and that around Mn in the quasicrystalline approximant α-AlMnSi suggests that their structures are well associated with that of the icosahedral quasicrystal.

4. Conclusion

The structure of $Zr_{80}Pt_{20}$ amorphous alloys was determined using the AXS-RMC method, and the obtained 3D structural model accurately reproduced the ordinary and environmental interference functions. Voronoi analysis indicated the overall preference for an icosahedral and icosahedral-like local structure around Pt, together with the strong chemical affinity of the Pt-Zr pair. CNA demonstrates the unique MRO of Pt-Pt, which is attributed to the connection of the SRO around Pt. The structural features around Pt are quite similar to those around Mn in α-AlMnSi. This similarity around Pt is suggested to be one of the factors responsible for the formation of the icosahedral phase during low temperature annealing.

Acknowledgments

The present AXS experiment was performed with the approval of the Photon Factory Advisory Committee (Proposal No. 2014G665). This work was financially supported in part by a Grant-in-Aid for Scientific Research (B) (16H04210) from the Japanese Society for the Promotion of Science (JSPS).

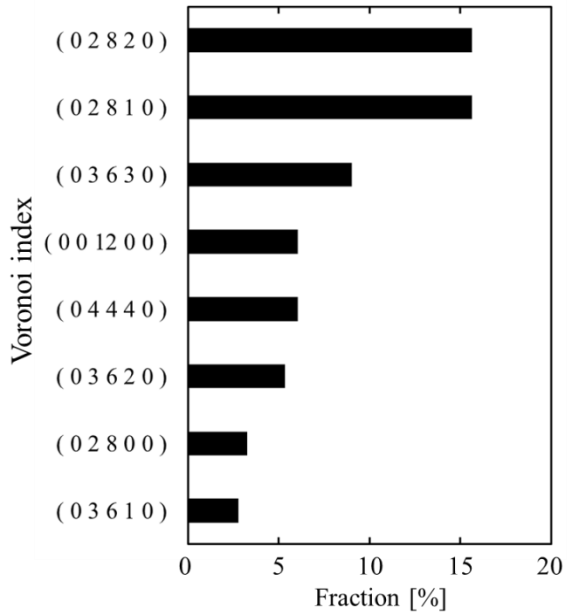

Figure 3. Frequency distribution of the typical Voronoi indices of Pt.

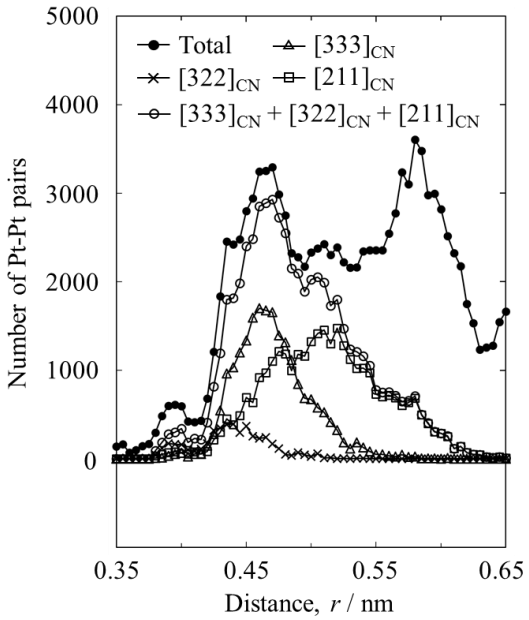

Figure 4. Results of CNA for the Pt-Pt root pairs in the MRO.

References

[1] Saida J, Imafuku M, Sato S, Matsubara E and Inoue A 2007 *J Non-Crsyt. Solids* **353** 3704.
[2] Saida J Matsushita M and Inoue A 2002 *J. Alloys Compd.* **342** 18.
[3] Saida J, Sunada T, Sato S, Imafuku M and Inoue A 2007 *Appl. Phys. Lett.* **91** 111901.
[4] Nakamura T, Matsubara E, Sakurai M, Kasai M, Inoue A and Waseda Y 2002 *J. Non-Cryst. Solids.* **312-314** 517.
[5] Sordelet D J, Ott R T, Wand S Y, Wang C Z, Besser M F, Liu A C Y and Kramer M J 2008 *Met. Mater. Trans.* **39A** 1908.
[6] Kawamata T, Yokoyama Y, Saito M, Sugiyama K and Waseda Y 2010 *Mater. Trans. Japan Inst. Metals* **51** 1796.
[7] Cromer D T and Liberman D 1970 *J. Chem Phys.* **53** 1891.
[8] Takeuchi A and Inoue A 2005 *Mater. Trans. Japan Inst. Metals* **46** 2817.
[9] Honeycutt J D and Anderson C 1987 J. Phys. Chem **91** 4950.
[10] Sugiyama K, Kaji N and Hiraga K 1998 Acta Crystallogr. **C54** 445.